Amidoximes: Promising Candidates for CO₂ Capture

Sonia Zulfiqar [a], Ferdi Karadas [b], Joonho Park [a], Erhan Deniz [b], Galen D. Stucky [c], Yousung Jung [a], Mert Atilhan [b] and Cafer T. Yavuz [a]

[a] *Graduate School of EEWS (WCU), Korea Advanced Institute of Science and Technology,, Daejeon 305-701, Republic of Korea*

[b] *Department of Chemical Engineering, Qatar University, PO Box: 2713, Doha, Qatar*

[c] *Department of Chemistry and Biochemistry, University of California, Santa Barbara, California 93106 – 5080, USA*

Supporting Information

# **Index**

A.   Theoretical Calculations

Both amidoxime and MEA have the same functional groups that can interact with carbon dioxide, amine and hydroxyl, but turn out to have somewhat different binding modes with different binding energetics. Ideally the CO_2 binding would occur with a concerted operation of the two functional groups simultaneously to maximize the adsorption. A different CO_2 removal mechanism of MEA (chemical absorption) and amidoxime (physical adsorption) makes a direct comparison of the efficiency of MEA and amidoxime for CO_2 capture less obvious theoretically. Nonetheless, the relative binding affinity of MEA and amidoximes for CO_2 would provide a useful guideline to explore new CO_2 scavengers. As a simple model, therefore, we have compared the CO_2 binding of methyl-MEA and acetamidoxime (AAO) using electronic structure calculations.

In a recent study of the zeolite imidazole framework (ZIF) interacting with CO_2, we have shown that electrostatic and dispersion interactions are both important to describe the CO_2/organic binding properly, and that the RIMP2 method captures both interactions reasonably well, hence used here too. The smaller VDZ(d) basis was used in geometry optimization and the larger cc-pVTZ basis was used for single point calculations to refine energetics. Basis set superposition error (BSSE) was corrected for all binding energies reported here using counterpoise correction. All calculations were performed using the Q-CHEM quantum chemistry package[1].

Among various conformers of the methyl-MEA/CO_2 complex, the gG conformer (Figure S1) is most stable (BE = 12.4 kJ/mol) where the capital G means the gauche form of the main dihedral (N-C-C-O), and the small g means the gauche form (-, counter clockwise) of lp-N-C-C (lp denotes the lone-pair of nitrogen)[2]. Here, upon complexation, CO_2 binds to the lone-pair of oxygen of the hydroxyl group and amine group helps the binding only indirectly via the internal H-bonding. During complexation, hydrogen moves toward nitrogen by 0.02 Å. This (partially indirect) conserted operation makes MEA better adsorbent than amine or hydroxyl group alone. In the second energy minimum structure (BE2 = 9.4 kJ/mol), CO_2 binds to both functional groups directly and simultaneously but with a smaller binding strength due to a loss of internal H-bonding.

BE1 = 12.4   BE2 = 9.4   BE3 = 8.8

(a) methyl-MEA

BE1 = 13.6   BE2 = 13.0   BE3 = 12.9
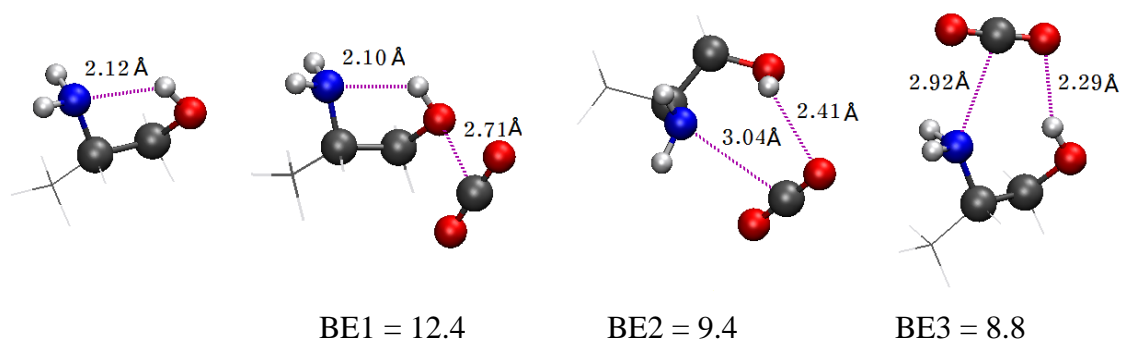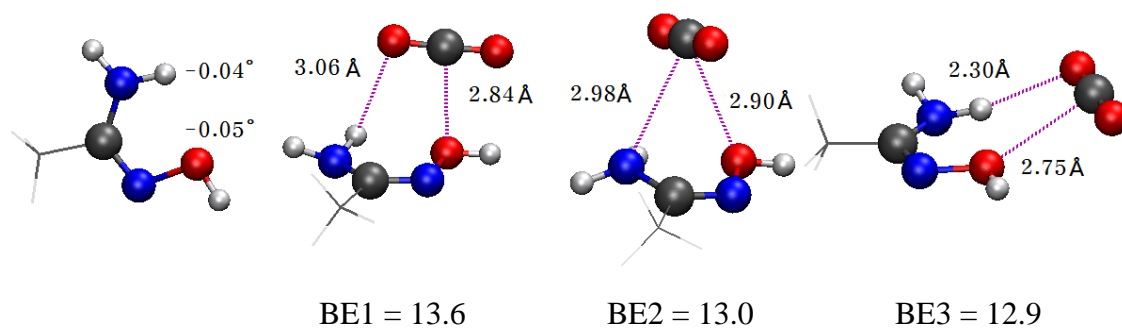
(b) AAO

Figure S1. The optimized structures with and without CO_2 for (a) methyl-MEA and (b) acetamidoxime (AAO) in the decreasing order of binding energy (BE1, BE2, BE3). Binding energies are in kJ/mol.

Amidoxime seems to be a stronger binder of CO_2 compared to MEA due to a planar structure that connects the two functional groups. Not only the -ON=CN- double bond ($\angle_{dihedral} = 0.05$), but also the =C-NH_2 group also has a planar structure ($\angle_{dihedral} = 0.04$). This implies that the lone-pair of nitrogen is in resonance with double bond. So all the atoms in the functional group makes a complete planar configuration which makes the interaction with CO_2 without much steric hinderance coming from numerous hydrogen atoms.

For amidoxime, therefore, CO_2 can bind roughly on the same amidoxime plane (i.e., -NC=NO-) or perpendicularly to it to interact with the two functional groups simultaneously. When CO_2 interacts normal to the amidoxime functional plane, two configurations are possible, one where the hydrogen of amine are attracted to CO_2 (BE1 = -13.6 kJ/mol) and the other where the lone-pair of nitrogen is attracted to CO_2 (BE2 = -13.0 kJ/mol). When CO_2 binds to amidoxime by side roughly on the same functional plane, it has a comparable BE with -12.9 kJ/mol. Optimized structures are shown in Figure S1. In all three configurations, CO_2 interacts with amidoxime via both functional group effectively, unlike in MEA where the lowest energy structure has an interaction with the hydroxyl group only.

B. Materials Synthesis and Characterization

1. Chemicals

Acetonitrile ($\geq$99.9%), terephthalonitrile (98%), polyacrylonitrile (Mw =150, 000), 7, 7, 8, 8-tetracyanoquinodimethane (98%), hydroxylamine solution (50 wt. % in H_2O) (99.9%), absolute ethanol ($\geq$99.8%) and n-hexane (95%) were procured from Aldrich and used as received.

2. Characterization

i. Melting Point Determination

Melting points of amidoximes were determined in capillary tubes using Electrothermal Melting Point Apparatus Model 9100.

ii. Elemental Analysis

C, H, N and O elemental analysis of amidoximes were performed using a Fisons EA 1108 and NA 2000 elemental analyzer.

iii. FT-IR Spectroscopy

Thin KBr pellets of all amidoximes were employed to record IR spectra over the range 4,000-550 cm^{-1} at a resolution of 4 cm^{-1} using FT-IR Spectrometer, Model No. FT-IR 4100 manufactured by Jasco.

iv. NMR Spectroscopy

The ^1H and ^{13}C NMR spectra of AAO, TPAO and TQAO were recorded on a Bruker AMX 500 MHz NMR Spectrometer in deuterated DMSO (DMSO-d_6). Tetramethylsilane was used as an internal reference. ^1H NMR and ^{13}C NMR spectra of PAO were not recorded due to its insolubility in deuterated solvents.

v. BET Analysis

Nitrogen adsorption–desorption isotherms were measured at 77 K using a Tristar 3020, Micromeritics (USA) porosimetry analyzer. For surface area determination, Brunauer–Emmett–Teller (BET) method was employed using a nitrogen molecule surface area of 0.162 nm^2.

3. Detailed Synthesis of Amidoximes

i. Acetamidoxime (AAO)

The synthesis of acetamidoxime was carried out in a dry 250 mL three-necked round bottom flask equipped with a magnetic stirrer and a thermocouple. Acetonitrile (0.02 mol) was charged into the reaction flask, followed by the addition of ethanol and the corresponding hydroxylamine solution (50 wt. % in H_2O) (0.022 mol) and stirred at 70°C for 7h. The completion of the reaction was verified by TLC until no starting material was present. The reaction mixture was highly transparent and colorless. The solvent was then removed under reduced pressure to yield the viscous residue and n-

hexane was added to this mixture and was kept in refrigerator for 30 min. The colorless needles like crystals obtained were dried under vacuum. Yield: 37 %; mp 134°C; Anal. Calcd for $C_2H_6N_2O$: C, 32.43; H, 8.16; N, 37.81; O, 21.60 %. Found: C, 32.45; H, 8.14; N, 37.78; O, 21.63 %. FTIR (KBr) 3491, 3370 cm^{-1} (N–H stretch), 3155 cm^{-1} (O–H stretch), 1398 cm^{-1} (C–N stretch), 1655 cm^{-1} (C=N stretch), 920 cm^{-1} (N–O stretch).). ^{1}H NMR: δ_H (500 MHz; DMSO-d_6) 5.42 (2H, s), 1.75 (3H, s), 8.66 (1H, s); ^{13}C NMR: δ_C (100 MHz; DMSO-d_6) 16.6, 149.5.

ii.   Terephthalamidoxime (TPAO)

Terephthalonitrile (0.02 mol) was dissolved in ethanol in a round bottom flask, and the hydroxylamine solution (50 wt. % in H_2O) (0.044 mol) was added with continuous stirring at 70°C for 2h. As the reaction proceeds, the contents of the flask first turned highly transparent and colorless and then after sometime precipitates appeared. The reaction was monitored by TLC until no starting material remained. The contents of the flask were centrifuged to isolate the precipitates which were then washed and dried under vacuum. Colorless rectangular plate shaped crystals were grown by slow evaporation from dimethyl sulfoxide solution. Yield: 81 %; mp 230°C; Anal. Calcd for $C_8H_{10}N_4O_2$: C, 49.48; H, 5.19; N, 28.85; O, 16.48 %. Found: C, 49.54; H, 5.16; N, 28.88; O, 16.42 %. FTIR (KBr) 3446, 3355 cm^{-1} (N–H stretch), 3223 cm^{-1} (O–H stretch), 1386 cm^{-1} (C–N stretch), 1649 cm^{-1} (C=N stretch), 928 cm^{-1} (N–O stretch).). ^{1}H NMR: δ_H (500 MHz; DMSO-d_6) 5.83 (2H, s), 7.66 (2H, s), 9.69 (1H, s); ^{13}C NMR: δ_C (100 MHz; DMSO-d_6) 126.3, 132.7, 154.2.
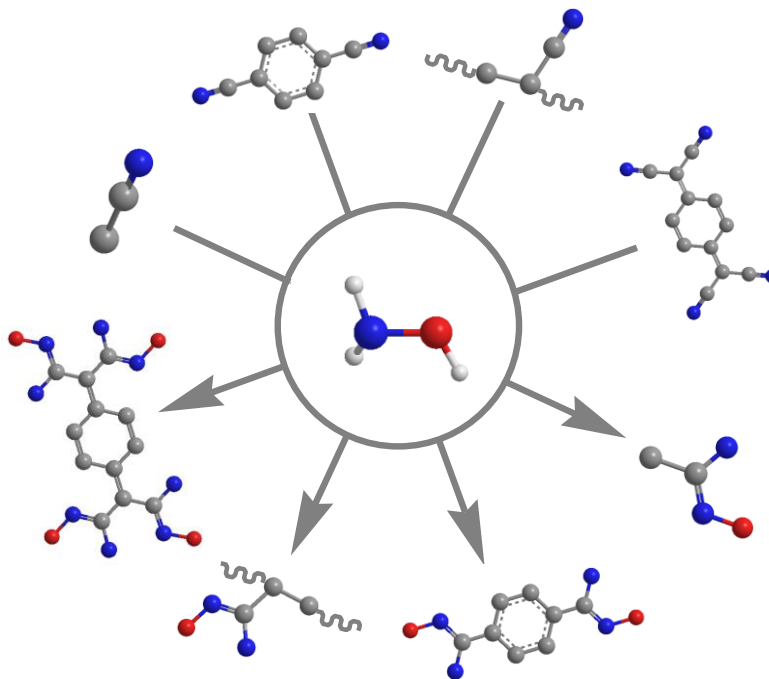
iii.   Polyamidoxime (PAO)

Polyacrylonitrile (1 mol) was dispersed in water followed by the addition of hydroxylamine solution (50 wt. % in H_2O) (1.1 mol) with uninterrupted agitation at 70°C for 4h. The reaction mixture was centrifuged to isolate the off-white colored product and dried under vacuum. Yield: 74 %; Anal. Calcd for $C_3H_6N_2O$: C, 41.85; H, 7.02; N, 32.54; O, 18.58 %. Found: C, 41.89; H, 6.99; N, 32.53; O, 18.59 %. FTIR (KBr) 3450, 3353 cm^{-}

^{1} (N–H stretch), 3200 cm^{-1} (O–H stretch), 1390 cm^{-1} (C–N stretch), 1654 cm^{-1} (C=N stretch), 931 cm^{-1} (N–O stretch).

iv. Tetraquinoamidoxime (TQAO)

In a round bottom flask, 0.02 moles of 7, 7, 8, 8-tetracyanoquinodimethane were placed followed by the addition of ethanol. The solution turned dark green then hydroxylamine solution (50 wt. % in H$_2$O) (0.088 mol) was added and mixture was stirred for 2 hr at 70°C and was checked by TLC. As reaction continues, there was formation of precipitates and the color of the solution changed to mustard. The light mustard colored product was collected and dried under vacuum. Yield: 65 %; mp 177°C; Anal. Calcd for C$_{12}$H$_{16}$N$_8$O$_4$: C, 42.86; H, 4.80; N, 33.32; O, 19.03 %. Found: C, 42.88; H, 4.79; N, 33.29; O, 19.04 %. FTIR (KBr) 3446, 3341 cm^{-1} (N–H stretch), 3197 cm^{-1} (O–H stretch), 1408 cm^{-1} (C–N stretch), 1655 cm^{-1} (C=N stretch), 918 cm^{-1} (N–O stretch). ^{1}H NMR: δ_H (500 MHz; DMSO-d$_6$) 5.55 (2H, s), 6.46 (1H, s), 9.41 (1H, s); ^{13}C NMR: δ_C (100 MHz; DMSO-d$_6$) 116.0, 126.4, 142.1, 179.5.

Figure S2. Synthesis of various amidoximes (Hydrogens are omitted for clarity).

4. Calculation of amidoxime functionality (%) of AAO, TPAO and TQAO

A typical amidoximation reaction

Amidoxime functional group

MW = 59.05
CH_3N_2O

AAO

MW = 74.08
$C_2H_6N_2O$

AO Functionality (%) = $\dfrac{59.05}{74.08}$ x 100

= 79.7%

TPAO

MW = 194.19
$C_8H_{10}N_4O_2$

AO Functionality (%) = $\dfrac{59.05 \text{ x } 2}{194.19}$ x 100

= 60.82%

TQAO

MW = 336.31
$C_{12}H_{16}N_8O_4$

AO Functionality (%) = $\dfrac{59.05 \text{ x } 4}{336.31}$ x 100

= 70.23%

C. CO₂ Adsorption Studies

Gravimetric carbon dioxide adsorption capacities of various amidoximes were studied at two different temperatures (43°C and 70°C) up to 180 bar using the high-pressure magnetic suspension balance (MSB) sorption device made by Rubotherm Präzisionsmesstechnik GmbH. MSB apparatus was kept at 100 °C up to 350 bars with two different operating positions. First, the measurement cell was filled with carbon dioxide at the sorption measurement position. MSB recorded the change in weight of the sample placed in the holder as the high pressure gas adsorbed on it. The second measurement position was used to measure the in-situ density of the high-pressure gas required to calculate the amount of the adsorbed gas on the solid sample in the high-pressure cell. Figure S3 shows the schematics of the MSB and its operating positions.

MSB measures the change in weight of a sorbent sample in the gravity field upon adsorption of molecules from a surrounding gas phase through contactless force transmission method; which enables much stable operations at high pressures. The weight gained by the sample within the high pressure cell is transmitted via contactless method using magnetic suspension coupling from a closed and pressure-proof metal container to an external microbalance. The measurement cell is equipped with platinum resistance thermometer Jumo DMM 5017 Pt100 that records temperature of the measuring cell within ± 0.6 °C accuracy. Pressure is monitored via Paroscientific® Digiquartz 745-3K with an accuracy of 0.01 %.

Typical measurements were carried out by placing 0.25 g of sample in the holder. At first the system was evacuated for 24 h at 60 °C. Carbon dioxide was then pressurized via Teldyne Isco 260D fully automated gas booster and charged into the high-pressure cell, where adsorption of carbon dioxide on the sample began. For each pressure point it took about 45 min to reach equilibrium (pressure and temperature) and once equilibrium was reached, 4 different set of measurements were taken for a period of 10 min; each data point was collected at every 30 sec. The total duration of each temperature and pressure point took about 50 min. At the end of each pressure point, system went to next pressure measurement point automatically. In this work, pressure up to 180 bars was used for maximum pressure and at the end of each isotherm, hysteresis check was conducted at each isotherm by collecting desorption data as the system was depressurized. Adsorption

data was analyzed and the amount of adsorbed carbon dioxide on the sample was calculated using the equation:

$$W + W_{buoy,sample} + W_{buoy,sink} = m_{ads} + m_{sample} + m_{sink} \qquad (1)$$

W = Signal read by the instrument

$W_{buoy,sample} = V_{sample} \times d_{gas}$ = Buoyancy correction due to sample

V_{sample} = volume of the sample

d_{gas} = Density of the gas

$W_{buoy,sink} = V_{sinker} \times d_{gas}$ = Buoyancy correction due to sinker

V_{sinker} = Volume of the sinker

m_{ads} = Adsorption amount

m_{sample} = Mass of the sample

m_{sink} = Mass of the sinker

$\mathbf{d_{gas}}$ was measured in-situ by means of the second measurement position (Figure S3). The mass of empty sinker was measured at several pressures of helium to determine the buoyancy due to sinker ($\mathbf{W_{buoy,sink}}$). Volume of the sinker ($\mathbf{V_{sinker}}$) was calculated from the slope of weight vs density plot obtained from this measurement. A blank measurement under vacuum was performed to determine the mass of sinker ($\mathbf{m_{sink}}$).

The buoyancy correction due to sample ($\mathbf{W_{buoy,sample}}$) was performed by calculating the volume of the sample ($\mathbf{V_{sample}}$), which is obtained by the slope of weight vs density plot obtained by a similar helium measurement of the sinker with the sample. Mass of the sample was determined by performing a measurement under vacuum. Activated Charcoal Norit® RB3 was used for calibration purpose to ensure the performance of MSB.

The CO_2 adsorption-desorption profile for each amidoxime was determined by exposing the sample to increasing and decreasing pressure increments of CO_2 gas at specific temperatures followed by evacuation. The sample and gas were allowed to come to equilibrium at each pressure point. The corresponding weight change was then corrected for buoyancy to obtain the adsorption amount (mmoles of CO_2/g of adsorbent).

Taking into account the polymeric structure and high surface area of PAO, CO_2 uptake was finally changed into mmoles of CO_2/m^2 of the adsorbent.
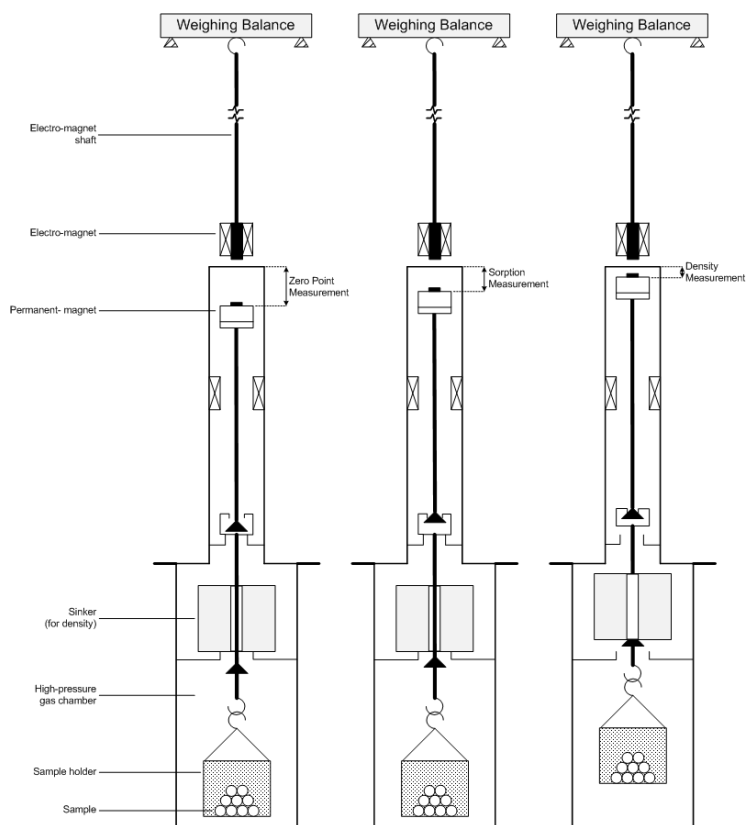
Figure S3. Schematics of MSB and its operation positions used for sorption and density measurements.

**Table S1. Surface area of various amidoximes and Norit RB3.**

Sample	BET Surface Area (m^2/g)
AAO	0.5875
TPAO	1.014
TQAO	5.401
PAO	8.674
AC Norit RB3	1100

Table S2. CO_2 Adsorption capacity (mmol/g) for different amidoximes at 180 bar.

Amidoxime	CO_2 Adsorbed (mmol/g) at 180 bar	
	T = 43°C	T = 70°C
AAO	1.64	2.71
TPAO	0.88	0.69
TQAO	1.63	1.36

Table S3. CO_2 Adsorption capacity $(mmol/m^2)$ for PAO and Norit RB3 at 180 bar.

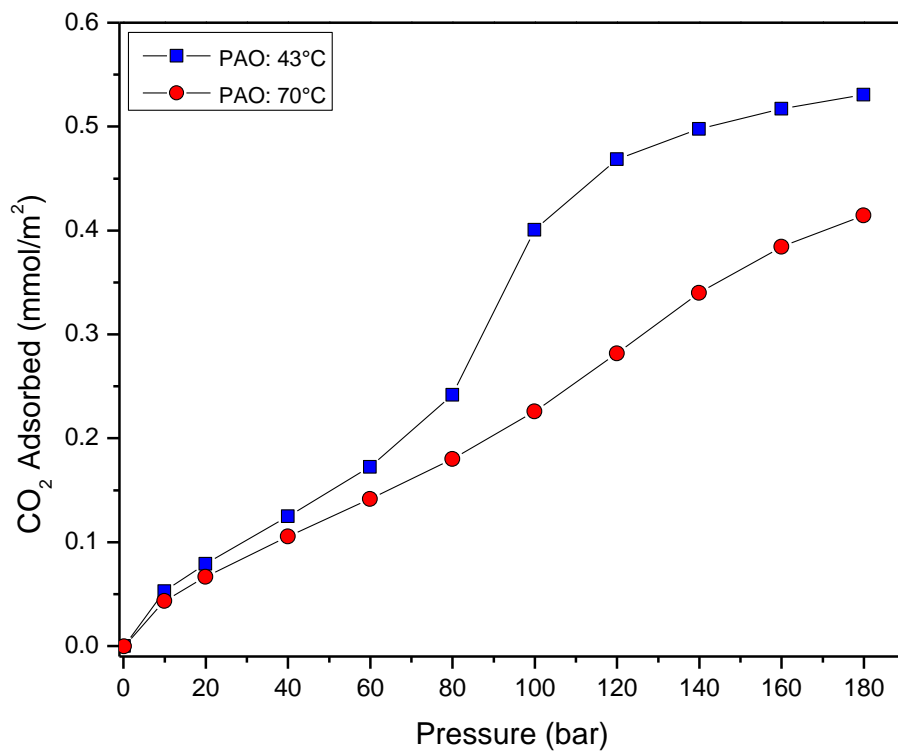| Amidoxime	CO_2 Adsorbed $(mmol/m^2)$ at 180 bar	
	T = 43°C	T = 70°C
PAO	0.53	0.41
AC Norit RB3	0.024	0.019
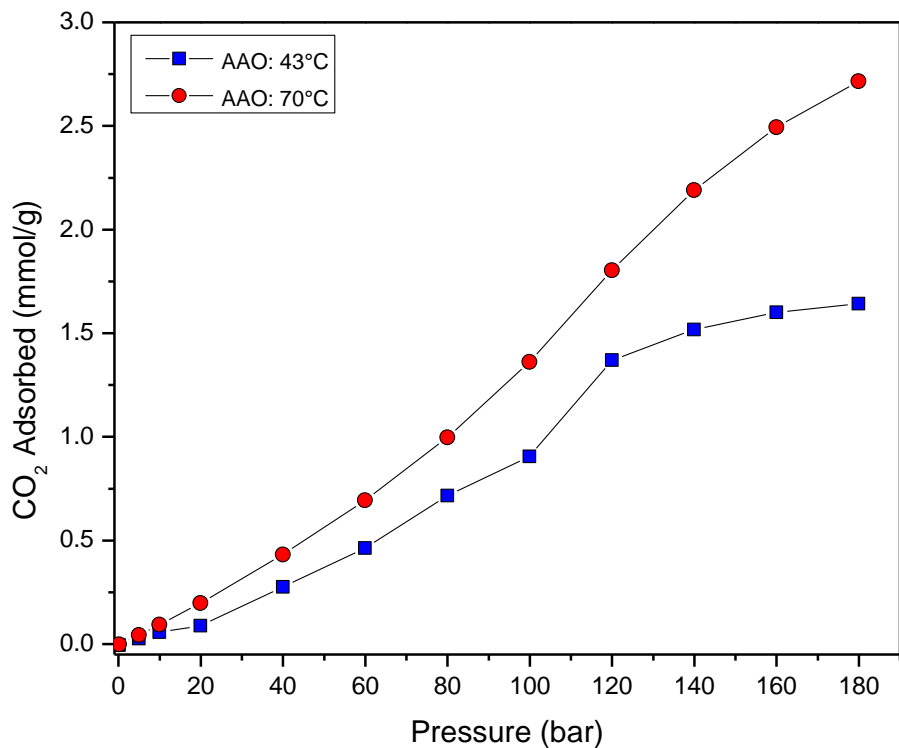
Figure S4. CO_2 adsorption isotherms (mmol/g) for AAO at 43°C and 70°C.
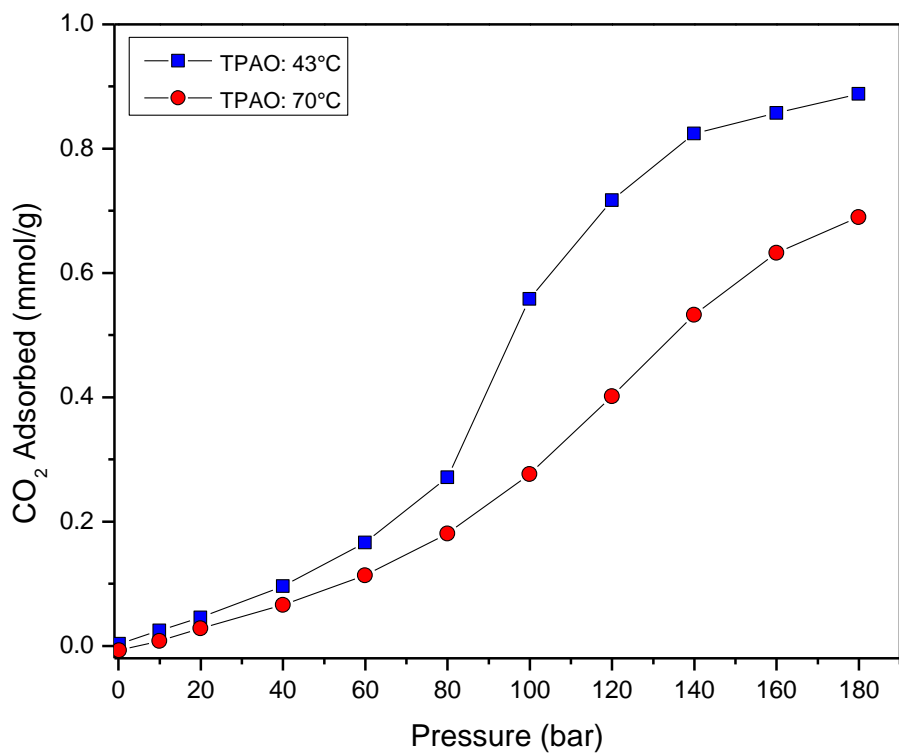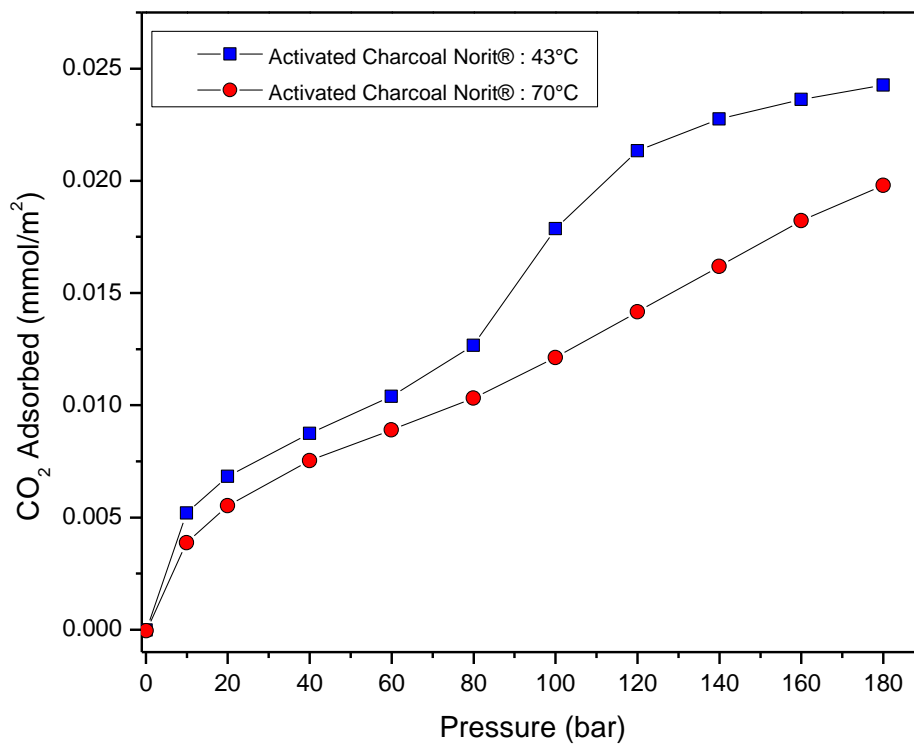

Figure S5. CO_2 adsorption isotherms (mmol/g) for TPAO at 43°C and 70°C.
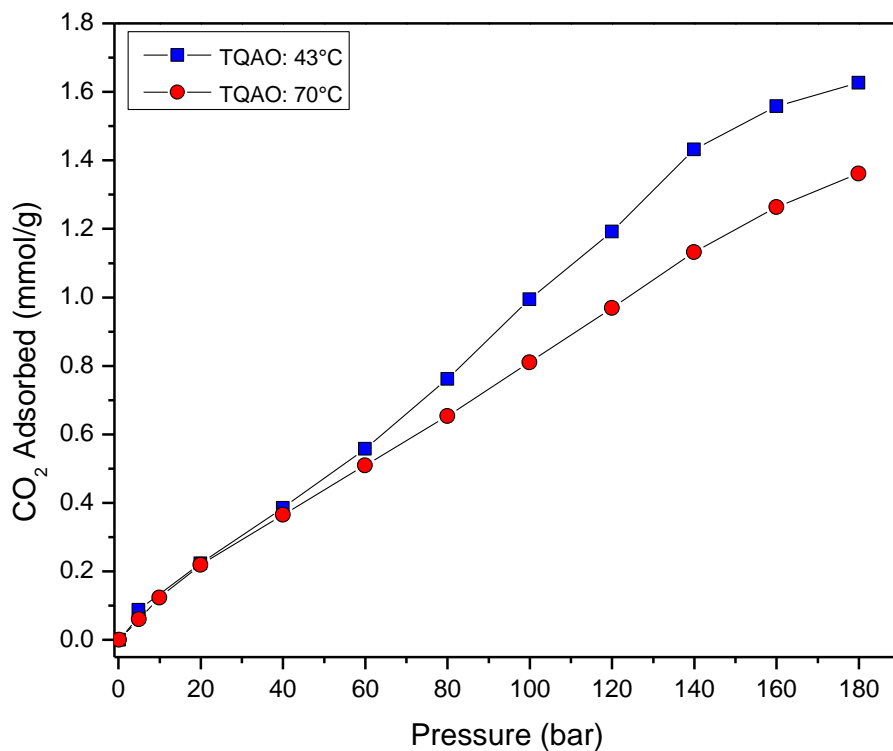
Figure S6. CO_2 adsorption isotherms (mmol/g) for TQAO at 43°C and 70°C.

Figure S7. CO_2 adsorption isotherms (mmol/m^2) for PAO at 43°C and 70°C.

Figure S8. CO_2 adsorption isotherms (mmol/m^2) for activated charcoal Norit RB3 at 43°C and 70°C.

D.   References

1. Y. Shao et al., *Phys. Chem. Chem. Phys.*, 2006, **8**, 3172.

2. I. Vorobyov, M. C. Yappert, and D. B. Dupre, *J. Phys. Chem.* A, 2002, **106**, 668.